GEOLOGY | THE GEOLOGICAL SOCIETY OF AMERICA®

https://doi.org/10.1130/G46734.1

Manuscript received 9 July 2019
Manuscript accepted 26 August 2019

Published online 15 October 2019

The origin of large gypsum crystals in the Geode of Pulpí (Almería, Spain)

A. Canals[1], A.E.S. Van Driessche[2], F. Palero[3] and J.M. García-Ruiz[3]*

[1]Department de Mineralogia, Petrologia i Geologia Aplicada, Facultat de Ciències de la Terra, Universitat de Barcelona, 08028 Barcelona, Spain

[2]Université Grenoble Alpes, Université Savoie Mont Blanc, CNRS, IRD, IFSTTAR, ISTerre, 38000 Grenoble, France

[3]Laboratorio de Estudios Cristalográficos, Instituto Andaluz de Ciencias de la Tierra, Consejo Superior de Investigaciones Científicas–Universidad de Granada, E-18100 Armilla, Granada, Spain

ABSTRACT

The Geode of Pulpí (Almería, Spain) is an ~11 m³ ovoid cavity, the walls of which are covered with meter-sized idiomorphic and highly transparent gypsum ($CaSO_4 \bullet 2H_2O$) crystals. We performed a thorough study based on field work, and petrographic and geochemical data collection, which aimed to reconstruct the geological history leading to the formation of this geode. The geode is hosted in mineralized Triassic carbonate rocks with a discontinuous mineral sequence from iron-carbonates and barite to celestine and finally gypsum (microcrystalline and selenite). Data from fluid inclusions show that barite precipitated above 100 °C, celestine at ~70 °C, and gypsum below 25 °C. All $\delta^{34}S$ sulfate phases fall between Triassic and Tertiary evaporite values. Barite and gypsum, either microcrystalline or large selenite crystals, show variable $\delta^{34}S$ and $\delta^{18}O$ compositions, whereas celestine and centimetric selenite gypsum have homogeneous values. We propose that the growth of the large selenite crystals in the Geode of Pulpí was the result of a self-feeding mechanism consisting of isovolumetric anhydrite replacement by gypsum at a temperature of 20 ± 5 °C, episodically contributed by a ripening process enhanced by temperature oscillations due to climatic change.

INTRODUCTION

One of the milestones of recent mineralogy has been the discovery of large gypsum crystals in different locations around the planet (García-Ruiz et al., 2008). Among them, the most spectacular is the Cave of Crystals in Naica (Mexico). However, there are other places with large selenite crystals that are interesting because of their beauty, such as the cave of crystals in the El Teniente mine (Chile) and the Geode of Pulpí (Spain), or due to their historical and archaeological interest, such as the mines of Lapis Specularis in Segóbriga (Spain; Bernárdez-Gómez and Guisado di Monti, 2007). Explaining the formation of these crystals is a challenge because they are the result of a process of crystal growth under conditions extremely close to equilibrium, i.e., in which time plays a key role, and therefore laboratory analogues are inefficient. Furthermore, with the exception of the natural laboratory of Naica, where the hydrothermal system is still active and some of the crystal growth conditions are still measurable (e.g., García-Ruiz et al., 2008; Van Driessche et al., 2019), most of the known locations where giant crystals of gypsum can be found are today hydrologically inactive.

In this paper, we focus on the Geode of Pulpí (Almería, Spain), an ~11 m³ ovoidal geode discovered in 1999 C.E. within the abandoned Mina Rica ("the Rich Mine"), in southeast Spain (Fig. 1; Palero et al., 2001). The walls are covered with large (~0.5 m), blocky selenite crystals of great transparency (Fig. 2). García-Guinea et al. (2002, p. 349) proposed that the crystals formed by the infiltration of an aqueous solution that "varied with time from freshwater in the earlier stages to seawater-like in later stages, most likely as a result of dissolution-recrystallization of earlier marine evaporites." Here, we present the results of detailed geological mapping of underground mining works together with a mineralogical and geochemical study of Mina Rica, with the aim to decipher the geological history leading to the formation of the large crystals in the geode.

GEOLOGICAL SETTING

The Mina Rica is located in the eastern part of the Betic Cordillera, the westernmost segment of the European Alpine belt, resulting from the early Cenozoic collision between the African and Eurasian plates. The mining complex is located in the east boundary of the Eastern Betic shear zone, which is still active and contributes to the deformation of this part of the Iberian Peninsula (Ortuño et al., 2012, and references therein). Specifically, the mine area is enclosed in a northeast-southwest dextral shear band overprinted by sinistral NNE-SSW faults, which are related to the Cocón-Terreros fault zone. This shear corridor extends beyond the domain of the mine toward the north and south, and it is partially covered by slope deposits (colluvial) from the Sierra del Aguilón (Fig. 1).

The complex structure of the Mina Rica can be described as a kilometer-scale lenticular bedding–carbonate competent body, bounded by two main subvertical northeast-southwest dextral faults and surrounded by less competent barren phyllites. Both lithologies are cut by dextral east-west and sinistral NNE-SSW and northwest-southeast faults (Fig. 1). The carbonate beds within the lens are arranged as steeply west-dipping NNE-SSW and northeast-southwest isoclinal folded sequences, forming wide bands bounded by NNE-SSW faults (Fig. DR1 in the GSA Data Repository[1]). These fractures

*E-mail: juanmanuel.garcia@csic.es

[1]GSA Data Repository item 2019396, supplementary information, including a geological sketch of the first level of the Mina Rica mine; isotope data; supplementary figures; fluid inclusions including methodological details and data; a table of isotopic composition; and U-Th age of carbonate speleothem, including experimental details, is available online at http://www.geosociety.org/datarepository/2019/, or on request from editing@geosociety.org.

CITATION: Canals, A., Van Driessche, A.E.S., Palero, F., and García-Ruiz, J.M., 2019, The origin of large gypsum crystals in the Geode of Pulpí (Almería, Spain): Geology, v. 47, p. 1161–1165, https://doi.org/10.1130/G46734.1

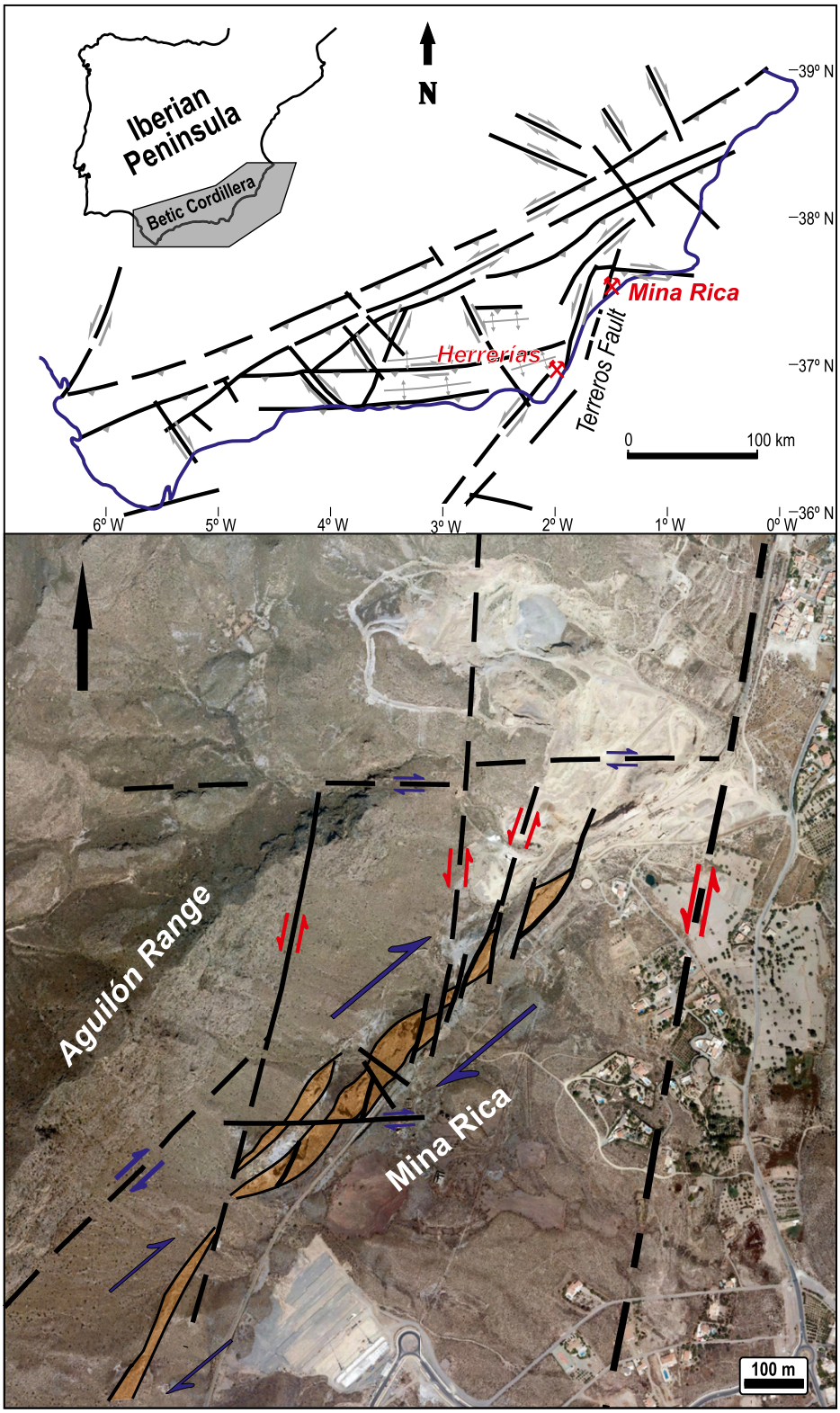

Figure 1. (Upper panel) Location of Mina Rica on the structural schema of the Betic Cordillera (Spain). (Lower panel) Zoom view showing main structures of the mine area; brown bodies correspond to carbonate lenses. Blue arrow structures are compatible with the Serravallian shear band, and red arrows correspond to Messinian reactivation and the Cocón-Terreros fault zone.

show evident signs of fragile reactivation, forming breccias. Cutting all these structures, there are two sets of open tension fractures, oriented northeast-southwest and NNW-SSE, which dip 60° east and 40° west, respectively.

Based upon their macroscopic appearance, we differentiated the following materials: barren phyllites, five carbonate units (mainly dolostone), microcrystalline gypsum, two breccia units, and Fe-carbonate ore bodies (Fig. DR1). Barren phyllites and carbonate rocks belong to the Triassic of the Alpujarride Complex described by Martin-Rojas et al. (2014), although their stratigraphic position and real thickness were not possible to establish because band distribution is bounded by faults. The microcrystalline gypsum packages, up to 5 m in thickness, are concordant with the bedded dolostones and belong to the stratigraphic pile; other microcrystalline, less continuous gypsums are younger in age, as they replace the ore carbonate (Fig. DR2A). One breccia unit corresponds to a mainly dedomitizated homolithic carbonate breccia with heterometric clasts up to meter size. Another gravitational collapse breccia filling a dissolution cavity is hosted in one of the microgypsum packages. The lithology of the breccia clasts corresponds to the surrounding rocks, both mineralized and nonmineralized (Fig. DR2C).

GEOLOGICAL HISTORY

The Mina Rica is a polymetallic (Pb-Zn-Fe-Ag) vein and manto deposit hosted in dolomitized Triassic rocks. This is a widespread base-metal–type deposit in the southeast of the Iberian Peninsula that is related to volcanic activity during the Miocene (Arribas and Tosdal, 1994). In Mina Rica, the first and main mineralization stage occurred after the Serravallian deformation (Sanz de Galdeano, 1990) and before 5.6 Ma. This upper time constraint, corresponding to the sea-level fall of the Messinian crisis, is based on the limit found by Dyja et al. (2015) for similar Fe-Ba mineralizations at Almagrera-Herrerías (Fig. 1). Siderite and ankerite replaced deformed carbonate rock with barite as a late phase. The multimodal distribution of homogenization temperatures (T_h) in barite fluid inclusions does not allow us to determine its growth temperature, although above 100 °C is plausible (see Fig. DR4). Barites have $\delta^{34}S$ (20.3‰ ± 0.6‰) and $\delta^{18}O$ (15.5‰ ± 0.8‰) compositions falling inside, or close to, the Tertiary marine box (Fig. 3A). In addition to the Triassic pile, anhydrite was present along with ore minerals.

A second mineralization stage is characterized by celestine ($SrSO_4$) forming fibrous ribbons around iron carbonate ores, and cementing breccias occurring in fragile structures produced by the reactivation of fractures related to Messinian compression described by Sanz de Galdeano (1990). The Messinian compression induced uplift of the area, leading to oxidation and dissolution of previous iron mineralization. The temperature decreased, and the water flooding the system induced dedolomitization and dissolution of anhydrite, both of which are known to release strontium (Al-Hashimi, 1976; Kaufman et al., 1990) and here triggered celestine precipitation. The few two-phase fluid inclusions found in celestine provide T_h data (from 63.0 °C to 74.4 °C) consistent with a low-temperature

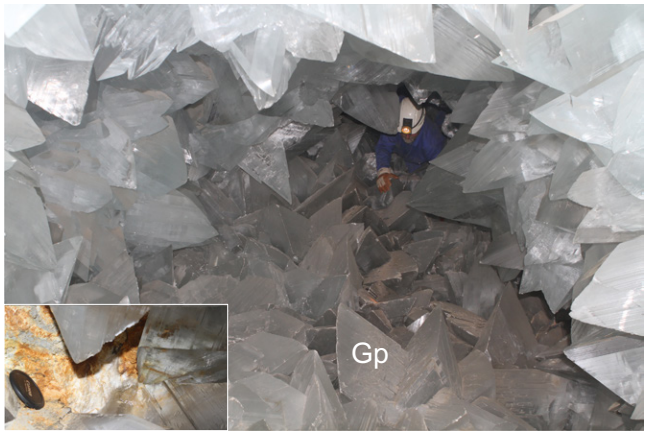

Figure 2. Geode of Pulpí (Almería, Spain). Lower inset is detailed view of the wall; notice how it is possible to see the wall through the crystals. Gray material is altered sulfides, mainly pyrite and marcasite. Gp—gypsum.

formation environment. Celestine shows homogeneous $\delta^{34}S$ values (20.0‰ ± 0.2‰) close to a Tertiary marine evaporite isotopic signature (Playà et al., 2000), and $\delta^{18}O$ values that vary from 15.0‰ to 17.6‰ (Fig. 3A). The area was located at that time in a marginal Messinian basin (Sissingh, 2008).

Once the strontium was exhausted, and the temperature decreased, microcrystalline gypsum was formed. Relics of anhydrite in the microcrystalline gypsum Triassic packages are still present (Fig. DR2B). While the major outcrops of microcrystalline gypsum that we mapped have homogeneous $\delta^{34}S$ values (+17.7‰ ± 0.2‰; gypsum A; Fig. 3A) and match values of Triassic evaporites in the Alpujarride Complex (Ortí et al., 2014), microcrystalline gypsum from less continuous outcrops shows higher and more scattered $\delta^{34}S$ values (+19.2‰ ± 0.6‰, gypsum B; see Fig. 3A). This last gypsum could have precipitated from the excess of calcium and sulfate, resulting not only from anhydrite dissolution, but isovolumetric anhydrite replacement by gypsum. Both sets of microcrystalline gypsum have a wider range of $\delta^{18}O$ values (between +13.7‰ and +17.3‰, and between +15.4‰ and 18.5‰; Fig. 3A).

As a result of the water flow along fragile structures, related either to early Pliocene uplift (Aguirre, 1998) or to Pleistocene vertical movements of the area (Boccaletti et al., 1987), gypsum was precipitated as centimeter-sized selenite crystals. All fluid inclusions in these gypsums are monophase, and, after laser-induced vapor phase treatment (Krüger et al., 2013), the measured T_h displayed a mean value of 17 ± 5.0 °C (Fig. 3B). The analyzed isotopic compositions ($\delta^{34}S$ = +18.8‰ ± 0.3‰ and $\delta^{18}O$ = +18.0‰ ± 0.4‰) are compatible with a dissolved sulfate source from the Triassic evaporite pile.

Inside the mine, scarce irregular decimeter pods of disseminated sulfides (Pb-Zn-Ag-Cu-Sn-Sb) are present. Some sulfides were formed after celestine and show a variable isotope composition ($\delta^{34}S$ from −6.6‰ to +9.9‰) compatible with local bacteriogenic sulfate reduction (Ehrlich et al., 2015). Moreover, evidence of oxidation of sulfides (mainly marcasite) was also observed. This could have acidified the water, leading to dissolution of the more permeable and reactive lithologies (dedolostone, homolithic breccias, and barren dolostone) and forming cavities that were later filled by heterolithic breccias. Barren carbonates, iron carbonates, celestine, and microcrystalline gypsum-anhydrite were found as clasts in these breccias (Fig. DR2C). Finally, at ca. 60 ka (U-Th age), the percolation of meteoric waters led to the formation of carbonated speleothems coating selenite crystals in the shallower levels of the mine. Thus, the selenite gypsum within the big geode was formed after the celestine stage and before the carbonate speleothems. The next section is a description of some singularities that help to propose a mechanism for their formation.

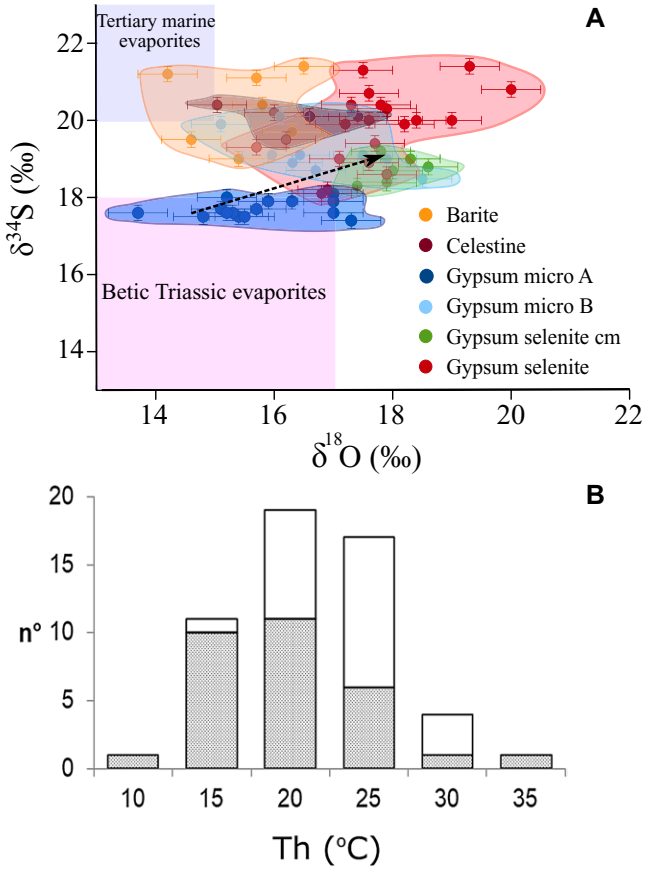

Figure 3. (A) Sulfur and oxygen isotope values obtained from sulfate minerals (barite, celestine and gypsum) retrieved from Mina Rica, southeast Spain (Table DR1 [see footnote 1]). Values for Triassic and Tertiary evaporites are from Ortí et al. (2014) and Playà et al. (2000), respectively. Line corresponds to isotopic fractionation between dissolved sulfate and gypsum at 20 °C (Van Driessche et al., 2016). (B) Temperature of homogenization (T_h) of fluid inclusions in selenite gypsum crystals; dots correspond to centimeter-size crystals.

FORMATION OF THE GEODE

There are several characteristics that indicate the Mina Rica selenite crystals formed from a calcium sulfate–rich solution at low supersaturation values. First, the small number of large crystals within the geode and their homogeneous size indicate an ultraslow nucleation flow, derived from a low supersaturation value maintained for a long time without large fluctuations. The longer crystal lying in the floor of the geode grew under the same conditions as the blocky crystals. The {100} contact twin indicates enhanced growth kinetics in the reentrance angle of the twin, demonstrating faster growth along the *c*-axis (Otálora and García-Ruiz, 2014). Second, the selenite crystals are transparent and pure, containing small amounts of impurities forming growth bands of solid inclusions at micrometer scales. Furthermore, we found continuity in grain size, coarsening from porphyroblastic to selenitic (Fig. DR3), and we recognized ghosts of gypsum grain boundaries in the selenitic crystals. Several mechanisms can be envisaged for the formation of supersaturated solutions of calcium sulfate, namely, thermal difference, salinity variation, and solubility differences among calcium sulfate phases.

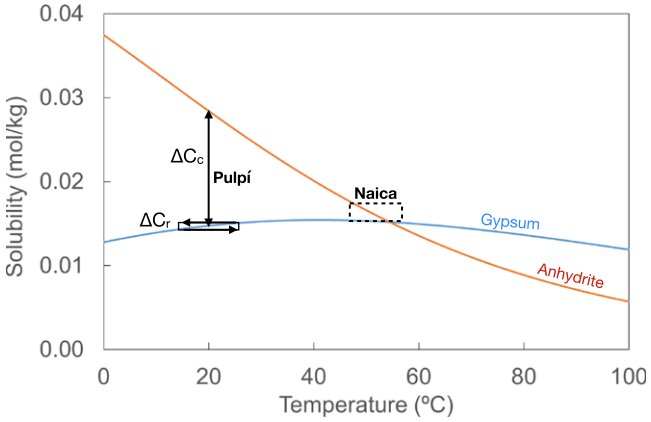

Figure 4. Variation of gypsum and anhydrite solubility with temperature. ΔC_c—concentration difference due to cooling; ΔC_r—concentration difference due to ripening. Dashed box corresponds to Naica (Mexico) gypsum crystal growth conditions (García-Ruiz et al., 2007). Solubility data were calculated with PHREEQC (version3.4.0, database phreeqc.dat) from Parkhurst and Appelo (2013).

The T_h values obtained from the analysis of selenite fluid inclusions showed that the growth temperature was much colder than the phase transition temperature for anhydrite/gypsum (~58 °C) and even colder than the temperature of maximum solubility of gypsum (~45 °C). This is also supported by the fact that, at room temperature, all the inclusions found in selenite crystals are monophase. Therefore, the formation of large crystals based on a slow cooling rate across the anhydrite/gypsum transition temperature, like the one accounting for the giant crystals of Naica, is very unlikely (Fig. 4).

Cooling from the temperature of maximum solubility of gypsum to the measured growth temperature (~20 °C) results in a difference of concentration that is too small (0.7 mmol/kg) to account for the massive crystallization of gypsum without a continuous external supply of calcium sulfate. Considering the variation in the solubility of calcium sulfate with NaCl, the mixing of freshwater and marine water, even if enriched in calcium and magnesium sulfate, does not lead to the formation of a supersaturated solution with respect to gypsum. Also, the significant variations in the isotope composition of selenite and microcrystalline gypsum suggest a local sulfate source rather than an external one (Fig. 3A). Therefore, it seems unavoidable that the crystals of the geode formed under a rather constant temperature around 20 °C. This could occur by the mechanism known as Ostwald ripening (Kahlweit, 1975; Chernov, 1984), a solution-mediated recrystallization under constant temperature by which the smaller gypsum crystallites in the mine will dissolve to feed the larger ones. However, Ostwald ripening of slightly soluble minerals like gypsum will yield, in the best of the cases, just a coarsening of the microcrystalline facies (Voorhees, 1985).

The efficiency of Ostwald ripening to account for the formation of large crystals is much enhanced when the smaller solid particles in the system are either amorphous or belong to an unstable polymorphic or hydrate phase (Steefel and Van Cappellen, 1990). This is the case at Mina Rica, because the presence of anhydrite triggered a self-feeding process, driven by the excess calcium and sulfate resulting from the isovolumetric anhydrite replacement by gypsum, and subsequent and concomitant gypsum growth. This mechanism works at a constant temperature within the range of temperature of the gypsum stability field and, along with ripening, would account for the slow growth rate leading to large crystals of high optical quality. In addition, the natural growth conditions at Pulpí provided another well-known mechanism that enhances ripening, namely, the existence of temperature oscillations (Mills et al., 2011), which, according to our measurements, would be around 20 ± 5 °C. These oscillations would be a reflection of the fluctuations of atmospheric temperature at a planetary scale (Hansen et al., 2013) and would occur provided that the growth environment remained underwater and was located relatively close to the surface. The low-temperature values of the fluid inclusions indicate that, at the time of the formation of the selenite crystals, the Mina Rica was located relatively close to the surface, and therefore its temperature was affected by climate changes.

ACKNOWLEDGMENTS

Financial support was provided by Projects CGL2010–16882 and CGL2010–12099-E (Ministerio de Educación y Ciencia [MEC]) and CGL2016–78971-P (MEC). We acknowledge logistic support from Magí Baselga, the Town Council of Pulpi, and the Junta de Andalucia (Proyecto de Excelencia RNM 5384). We are grateful to Yves Krüger for his assistance during monophase inclusion measurements. Van Driessche acknowledges funding from the French national program EC2CO–Biohefect, SULFCYCLE.

REFERENCES CITED

Aguirre, J., 1998, El Plioceno del SE de la Península Ibérica (Provincia de Almería): Síntesis estratigráfica, sedimentaria, bioestratigráfica y paleogeográfica: Revista de la Sociedad Geologica de España, v. 11, p. 297–315.

Al-Hashimi, W.S., 1976, Significance of strontium distribution in some carbonate rocks in the Carboniferous of Northumberland, England: Journal of Sedimentary Research, v. 46, p. 369–376.

Arribas, A., and Tosdal, R.M., 1994, Isotopic composition of Pb in ore-deposits of the Betic Cordillera, Spain: Origin and relationship to other European deposits: Economic Geology and the Bulletin of the Society of Economic Geologists, v. 89, p. 1074–1093, https://doi.org/10.2113/gsecongeo.89.5.1074.

Bernárdez-Gómez, M.J., and Guisado di Monti, J.C., 2007, Las referencias al *lapis specularis* en la Historia Natural de Plinio el Viejo: Pallas, v. 75, p. 49–57.

Boccaletti, M., Gelati, R., López Garrido, A.C., Papani, G., Rodríguez Fernández, J., and Sanz de Galdeano, C., 1987, Neogene–Quaternary sedimentary-tectonic evolution of the Betic Cordillera: Acta Naturalia de l'Ateneo Parmense, v. 23, p. 179–200.

Chernov, A.A., 1984, Modern Crystallography III: Crystal Growth: Berlin, Springer, 517 p., https://doi.org/10.1007/978-3-642-81835-6.

Dyja, V., Hibsch, C., Tarantola, A., Cathelineau, M., Boiron, M.C., Marignac, C., Bartier, D., Carrillo-Rosúa, J., Morales-Ruano, S., and Boulvais, P., 2015, From deep to shallow fluid reservoirs: Evolution of fluid sources during exhumation of the Sierra Almagrera, Betic Cordillera, Spain: Geofluids, v. 16, p. 103–128, https://doi.org/10.1111/gfl.12139.

Ehrlich, H.L., Newman, D.K., and Kappler, A., 2015, Ehrlich's Geomicrobiology (6th ed.): Boca Raton, Florida, CRC Press, 635 p., https://doi.org/10.1201/b19121.

García-Guinea, J., Morales, S., Delgado, A., Recio, C., and Calaforra, J.M., 2002, Formation of gigantic gypsum crystals: Journal of the Geological Society [London], v. 159, p. 347–350, https://doi.org/10.1144/0016-764902-001.

García-Ruiz, J.M., Villasuso, R., Ayora, C., Canals, A., and Otarola, F., 2007, Formation of natural gypsum megacrystals in Naica: Geology, v. 35, p. 327–330, https://doi.org/10.1130/G23393A.1.

García-Ruiz, J.M., Canals, A., and Ayora, C., 2008, Gypsum megacrystals, *in* McGraw-Hill Yearbook of Science and Technology: New York, McGraw-Hill, p. 154–156.

Hansen, J., Sato, M., Russell, G., and Kharecha, P., 2013, Climate sensitivity, sea level and atmospheric carbon dioxide: Philosophical Transactions of the Royal Society, ser. A, v. 371, p. 20120294, https://doi.org/10.1098/rsta.2012.0294.

Kahlweit, M., 1975, Ostwald ripening of precipitates: Advances in Colloid and Interface Science, v. 5, p. 1–35, https://doi.org/10.1016/0001-8686(75)85001-9.

Kaufman, J., Meyers, W.J., and Hanson, G.N., 1990, Burial cementation in the Swan Hills Formation (Devonian), Rosevear Field, Alberta, Canada: Journal of Sedimentary Research, v. 60, p. 918–939.

Krüger, Y., García-Ruiz, J.M., Canals, À., Marti, D., Frenz, M., and Van Driessche, A.E., 2013, Determining gypsum growth temperatures using monophase fluid inclusions—Application to the giant gypsum crystals of Naica, Mexico: Geology, v. 41, p. 119–122, https://doi.org/10.1130/G33581.1.

Martin-Rojas, I., Somma, R., Estévez, A., Delgado, F., and Zamparelli, V., 2014, La plataforma Triásica Alpujárride (Zonas internas de la Cordillera Bética, España): Revista de la Sociedad Geológica de España, v. 27, p. 63–78.

Mills, R.D., Ratner, J.J., and Glazner, A.F., 2011, Experimental evidence for crystal coarsening and fabric development during temperature cycling: Geology, v. 39, p. 1139–1142, https://doi.org/10.1130/G32394.1.

Ortí, F., Pérez-López, A., García-Veigas, J., Rosell, L., Cendón, D.I., and Pérez-Valera, F., 2014, Sulfate isotope compositions ($\delta^{34}S$, $\delta^{18}O$) and strontium isotopic ratios ($^{87}Sr/^{86}Sr$) of Triassic

evaporites in the Betic Cordillera (SE Spain): Revista de la Sociedad Geológica de España, v. 27, p. 79–89.

Ortuño, M., Masana, E., García-Meléndez, E., Martínez-Díaz, J.J., Stepancikovà, P., Cunha, P.P., Sohbati, R., Canora, C., Buylaert, J.P., and Murray, A.S., 2012, An exceptionally long paleoseismic record of a slow-moving fault: The Alhama de Murcia fault (Eastern Betic shear zone, Spain): Geological Society of America Bulletin, v. 124, p. 1474–1494, https://doi.org/10.1130/B30558.1.

Otalora, F., and García-Ruiz, J.M., 2014, Nucleation and growth of the Naica giant gypsum crystals: Chemical Society Reviews, v. 43, p. 2013–2026, https://doi.org/10.1039/C3CS60320B.

Palero, F.J., Gómez, F., and Cuesta, J.M., 2001, Pilar de Jaravía: La Geoda Gigante de la Mina Rica: Bocamina, v. 6, p. 54–67.

Parkhurst, D.L., and Appelo, C.A.J., 2013, Description of input and examples for PHREEQC version 3—A computer program for speciation, batch-reaction, one-dimensional transport, and inverse geochemical calculations: U.S. Geological Survey Techniques and Methods, Book 6, 497 p., https://pubs.usgs.gov/tm/06/a43/.

Playà, E., Ortí, F., and Rosell, L., 2000, Marine to non-marine sedimentation in the Upper Miocene evaporites of the Eastern Betics, SE Spain: Sedimentological and geochemical evidence: Sedimentary Geology, v. 133, p. 135–166, https://doi.org/10.1016/S0037-0738(00)00033-6.

Sanz de Galdeano, C., 1990, Geologic evolution of the Betic Cordilleras in the Western Mediterranean, Miocene to the present: Tectonophysics, v. 172, p. 107–119, https://doi.org/10.1016/0040-1951(90)90062-D.

Sissingh, W., 2008, Punctuated Neogene tectonics and stratigraphy of the African-Iberian plate-boundary zone: Concurrent development of Betic-Rif basins (southern Spain, northern Morocco): Netherlands Journal of Geosciences, v. 87, p. 241–289, https://doi.org/10.1017/S0016774600023350.

Steefel, C.I., and Van Cappellen, P., 1990, A new kinetic approach to modeling water-rock interaction: The role of nucleation, precursors, and Ostwald ripening: Geochimica et Cosmochimica Acta, v. 54, p. 2657–2677, https://doi.org/10.1016/0016-7037(90)90003-4.

Van Driessche, A.E.S., Canals, A., Ossorio, M., Reyes, R.C., and García-Ruiz, J.M., 2016, Unraveling the sulfate sources of (giant) gypsum crystals using gypsum isotope fractionation factors: The Journal of Geology, v. 124, p. 235–245, https://doi.org/10.1086/684832.

Van Driessche, A.E.S., Stawski, T.M., and Kellermeier, M., 2019, Calcium sulfate precipitation pathways in natural and engineered environments: Chemical Geology, https://doi.org/10.1016/j.chemgeo.2019.119274.

Voorhees, P.W., 1985, The theory of Ostwald ripening: Journal of Statistical Physics, v. 38, p. 231–252, https://doi.org/10.1007/BF01017860.

Printed in USA